Geophysical Research Letters

RESEARCH LETTER
10.1029/2020GL089134

Convective Invigoration Traced to Warm-Rain Microphysics

Xin Rong Chua[1,2] **and Yi Ming**[1,3]

[1]Program in Atmospheric and Oceanic Sciences, Princeton University, Princeton, NJ, USA, [2]Now at Centre for Climate Research Singapore, Singapore, [3]Geophysical Fluid Dynamics Laboratory/NOAA, Princeton, NJ, USA

Key Points:
- Higher cloud droplet number concentration increases convective mass flux, even in the absence of ice microphysics
- The convective invigoration coincides with higher tropospheric relative humidity and reevaporation efficiency
- The dynamical mechanism involves a vertical dipole (cooling-above-warming) pattern

Supporting Information:
- Supporting Information S1

Correspondence to:
Y. Ming,
Yi.Ming@noaa.gov

Citation:
Chua, X. R., & Ming, Y. (2020). Convective invigoration traced to warm-rain microphysics. *Geophysical Research Letters*, *47*, e2020GL089134. https://doi.org/10.1029/2020GL089134

Received 20 JUN 2020
Accepted 28 OCT 2020
Accepted article online 9 NOV 2020

Abstract Aerosols are postulated to alter moist convection by increasing cloud droplet number concentration (N_d). Cloud-resolving model simulations of radiative-convective equilibrium show that higher N_d leads to stronger convective mass flux, seemingly in line with a hypothesis that links the convective invigoration to delayed rain formation allowing more cloud liquid condensate to be frozen. Yet, the invigoration is also present in an alternative model configuration with warm-rain microphysics only, suggesting that ice microphysics is not central to the phenomenon. The key dynamical mechanism lies in the different vertical distributions of the increases in water vapor condensation and in cloud liquid reevaporation, causing a dipole pattern favoring convection. This is further supported by a pair of mechanism-denial experiments in which an imposed weakening of cloud liquid reevaporation tends to mute invigoration.

Plain Language Summary Aerosols are thought to affect moist convection by increasing cloud droplet number concentration. According to a popular hypothesis, higher droplet number concentration would delay rain formation, allowing more cloud water to reach the freezing level. The additional latent heating from freezing is presumed to cause stronger convection. We test this hypothesis with a numerical model capable of simulating moist convection, and find that convective invigoration occurs even in the absence of ice processes. A detailed analysis suggests that the slowdown of rain formation increases cloud liquid reevaporation. The resulting cooling is balanced primarily by stronger water vapor condensation. This creates a vertical cooling-above-warming dipole pattern favorable to convection.

1. Introduction

Aerosols, natural and anthropogenic alike, alter Earth's radiative budget by scattering and/or absorbing shortwave radiation, as well as by altering cloud albedo (Twomey, 1974) and lifetime (Albrecht, 1989). Both effects have important implications for moist convection and precipitation. This work focuses on the purely microphysical pathway through which aerosols affect deep convective clouds by increasing cloud droplet number concentration (N_d). A commonly referenced mechanism (Andreae et al., 2004; Rosenfeld et al., 2008; Williams et al., 2002) posits that higher N_d leads to smaller droplets, thus delaying rain formation. This effect tends to bring more cloud liquid water above the freezing level, and the additional latent heat release would invigorate convection.

Stevens and Feingold (2009) hypothesized that delayed precipitation formation would allow more liquid to reach the cloud-top region of a cumulus. The resulting reevaporative cooling has an effect of destabilizing the atmospheric column, and thus promoting convection, consistent with the results of Xue and Feingold (2006) and Jiang and Feingold (2006). It was also suggested that the subsequent increase in the precipitation efficiency of deep clouds could buffer the initial suppression of precipitation (Seifert et al., 2015). More broadly, the reevaporation of cloud condensate, by influencing cold pool strength, can exert a strong control on subsequent convection (e.g., Morrison, 2012; Tao et al., 2007, 2012). A recent study by Fan et al. (2018) suggested that ultrafine aerosol particles (smaller than 50 nm) can be activated into cloud droplets in a clean environment owing to higher in-cloud supersaturation; the additional droplets in return facilitate condensation. It was argued that the resulting convective invigoration occurs via a warm-phase (liquid) microphysical pathway based on the relatively small increase in upper-level latent heating. In other words, one does not have to rely on ice microphysics to explain the convective adjustment to aerosols.

To further complicate the matter, there is no consensus among the existing case studies on how aerosols would strengthen or weaken convection (see Morrison, 2012 for a case of weakening). It is not straightforward to make comparison across different case studies given that environmental factors such as wind shear (e.g., Fan et al., 2009) and cloud-radiative effects (e.g., Fan et al., 2015) can potentially alter the eventual convective response. In contrast, the setting of radiative-convective equilibrium (RCE) makes it possible to diagnose which processes are of leading-order importance to the simulated quasi-steady state in a simple framework. For example, van den Heever et al. (2011) found an increase in the frequency of updrafts in response to increased N_d. In a follow-up study focusing on deep convective clouds, Storer and van den Heever (2013) showed that the freezing of cloud liquid is not among the largest contributors to the overall latent heat budget, suggesting that at least in RCE, freezing might not be as important for understanding convective invigoration as initially thought. This study is conceived as a targeted mechanistic study of the role of liquid microphysics in determining aerosol effects on convection.

2. Methodology

The RCE simulations are performed with the Weather Research and Forecasting (WRF) model (Wang & Sobel, 2011), a widely used cloud-resolving model (CRM). The configuration is identical to that used in Chua et al. (2019) except for the treatment of cloud microphysics (as detailed later). The model domain is doubly periodic and contains 96 × 96 grid points at a horizontal resolution of 2 km with 50 vertical levels. Atmospheric radiative cooling is prescribed at $-1.5\,\mathrm{K\,day^{-1}}$ in the troposphere (defined as temperature warmer than 207.5 K). Elsewhere temperature is relaxed to 200 K over 5 days following a Newtonian relaxation scheme. Prescribing radiative cooling eliminates a major confounding factor common to this type of studies. Surface sensible and latent heat fluxes are computed with an aerodynamic formulation at a constant near-surface wind speed of $5\,\mathrm{m\,s^{-1}}$. The surface temperature is set at 301.15 K. Subgrid diffusion is calculated with the Smagorinsky and YSU schemes (Hong et al., 2006). Domain-average winds are nudged to 0 on a time scale of two hours.

The model uses the double-moment Morrison cloud microphysics scheme (Morrison et al., 2009). By tracking both mass mixing ratios and numbers of hydrometeors, a double-moment scheme is deemed to be more suitable for simulating the microphysical effects of aerosols on moist convection than a single-moment scheme of mixing ratios. The warm-rain or liquid part of the scheme is described briefly here as it is important for understanding the results. Water vapor (q_v) condenses into cloud liquid (q_l) through saturation adjustment. Note that q denotes mass mixing ratio. Reevaporation of cloud liquid occurs only under subsaturated conditions. Cloud liquid converts into rain (q_r) through either autoconversion or accretion; the rates are parameterized as $1{,}350\,q_l^{2.47}N_d^{-1.79}$ and $67(q_l q_r)^{1.15}$, respectively (Khairoutdinov & Kogan, 2000). Note that q_l and q_r are in $\mathrm{kg\,kg^{-1}}$, N_d in $\mathrm{cm^{-3}}$, and the rates in $\mathrm{kg\,kg^{-1}\,s^{-1}}$. Autoconversion is the only microphysical process that is controlled directly by N_d. Rain can reevaporate back into water vapor.

Three alternative configurations are created from simplifying the full model (referred to as FU). One can turn off the ice part of the Morrison scheme. In the resulting configuration (referred to as LI), the liquid microphysics operates at all temperatures. The formulae used for computing the cloud liquid and rain reevaporation rates are scaled by a factor of 0.1 in the CE and RE configurations, respectively. This does not mean that the actual rates would decrease by 10 times as other factors may also vary.

For each of the four model configurations (i.e., FU, LI, CE, and RE), a pair of simulations are performed. N_d is set to $100\,\mathrm{cm^{-3}}$ in the control experiment, and $1{,}000\,\mathrm{cm^{-3}}$ in the perturbation experiment. The former is denoted by the name of a configuration, and the latter by adding an asterisk. For example, the control and perturbation experiments performed with the full model are referred to as FU and FU*, respectively.

A control experiment is initialized from a warm bubble, and is integrated for 240 model days. The output at Day 180 is used to initialize a corresponding 60-day perturbation experiment. We analyze the last 20 days of hourly-mean outputs from each simulation. The noise level of a given variable is quantified using five consecutive, nonoverlapping 20-day periods from an extended full model control simulation (namely, FU).

3. Results

Some key characteristics of the control simulations and their changes in response to higher N_d are depicted in Figure 1. The distributions of cloud liquid (q_l) in the lower and midtroposphere are similar among all

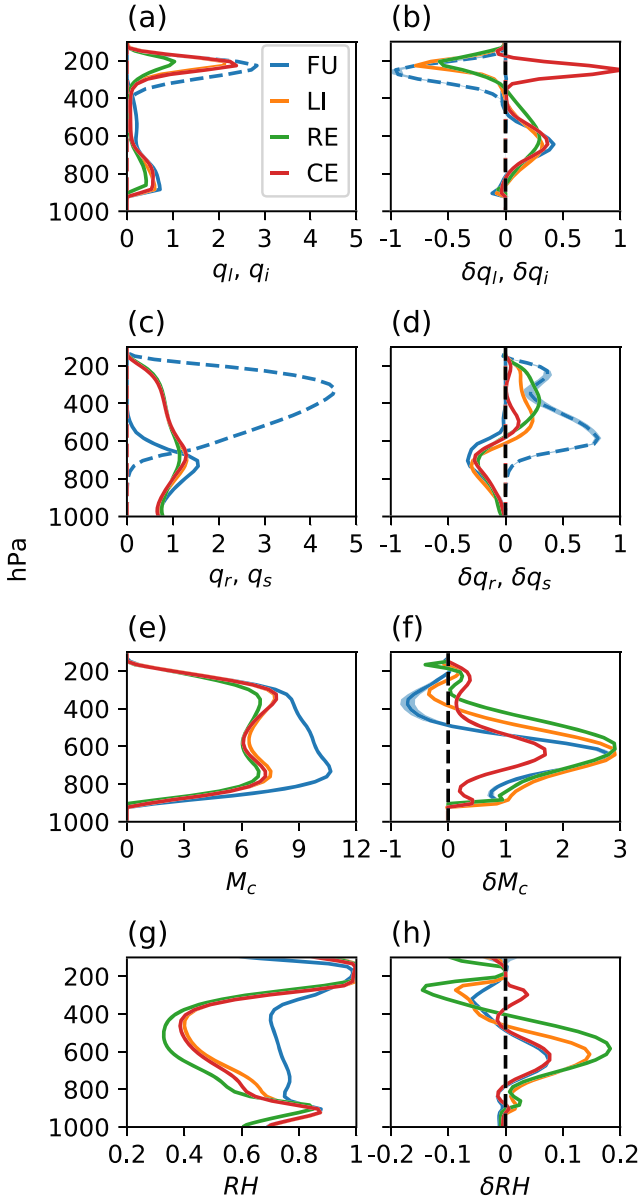

Figure 1. Vertical profiles of the domain-average (a and b) cloud liquid (solid, q_l, 10^{-5} kg^{-1} kg^{-1}) or ice (dashed, q_i, 10^{-5} kg^{-1} kg^{-1}) mixing ratio, (c and d) rain (solid, q_r, 10^{-5} kg^{-1} kg^{-1}) or snow (dashed, q_s, 10^{-5} kg^{-1} kg^{-1}) mixing ratio, (e and f) convective mass flux (M_c, g m^{-2} s^{-1}), and (g and h) relative humidity (RH, unitless). The control experiments are in the left column, and the difference between the control and perturbation experiments are in the right column. The shading denotes the noise levels in FU. Note that cloud ice and snow are present only in FU and FU*.

four configurations, with a distinct peak at around 900 hPa (Figure 1a). As designed, high clouds are composed of ice (q_i) in FU, and liquid in the other cases. Interestingly, the upper-tropospheric q_l in LI and CE is comparable to q_i in FU, but much higher than q_l in RE. Higher N_d gives rise to an increase in cloud condensate below 500 hPa in all cases (Figure 1b). CE is opposite to the other three cases in showing a substantial increase in high cloud condensate.

In FU, rain (q_r) is concentrated mostly below 500 hPa, while snow and graupel (collectively referred to as snow, q_s) dominates above, a vertical partitioning similar to that in Heikenfeld et al. (2019). The three liquid microphysics control simulations exhibit almost identical vertical distributions of rain throughout the column, which are bottom heavy with maxima at around 700 hPa (Figure 1c). Elevated N_d causes q_r to decrease in all cases below 600 hPa, and to increase in the three liquid microphysics cases above, albeit to varying degrees (Figure 1d). q_s in FU increases as well. Taken together, the increase in cloud liquid and the

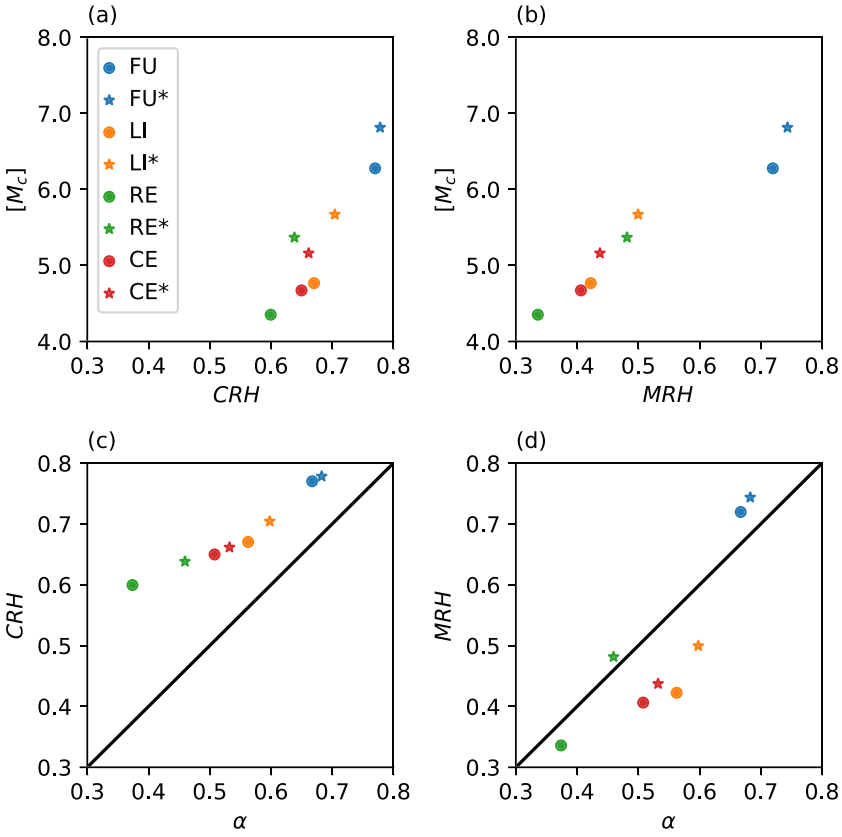

Figure 2. Scatter plots of (a) vertically averaged convective mass flux ([M_c], g m^{-2} s^{-1}) versus column relative humidity (*CRH*,unitless), (b) [M_c] versus midtropospheric (400 to 600 hPa) relative humidity (*MRH*, unitless), (c) *CRH* versus the reevaporation ratio (α, unitless), and (d) *MRH* versus α in all experiments.

concurrent decrease in rain in the lower troposphere are consistent with the microphysical nature of the perturbation, that is, higher N_d tending to suppress the conversion of cloud liquid to rain, while convective adjustment seems to play a prominent role in shaping the upper-tropospheric changes.

We quantify convective invigoration by convective mass flux (M_c), computed by summing the mass flux at grid points where the total cloud condensate (q_c, or $q_l + q_i$) is greater than 0.005 g kg^{-1} and vertical velocity exceeds 1 m s^{-1} (Wang & Sobel, 2011). In much of the troposphere, M_c in FU is substantially (about 40%) stronger than in the liquid microphysics cases (Figure 1e). They also differ in vertical structures; FU has only one in the lower troposphere, while the latter have two peaks, one in the lower troposphere and the other in the upper troposphere. M_c shows a substantial increase below 500 hPa due to higher N_d, which amounts to ~30% at 600 hPa (Figure 1f). The convective invigoration is accompanied by a relatively small decrease in M_c in the upper troposphere in FU* and LI*. The magnitude of the enhancement of M_c is fully captured in LI, suggesting that ice microphysics is not essential for explaining the convective invigoration, contrary to Rosenfeld et al. (2008). Furthermore, the invigoration is muted in the configuration of CE, indicating that cloud liquid reevaporation may be a key process involved in the convective response. In contrast, RE does not show any appreciable difference from LI, which hints at a secondary role played by rain reevaporation. Self-aggregation does not occur in the simulations examined here, as one might expect from the relatively small domain size.

Figure 1g shows the relative humidity (*RH*) in the control cases. The vertical profiles take a C shape, with minima at around 500 hPa. FU, however, has notably higher mid-tropospheric *RH* (~0.7) than the liquid microphysics cases (~0.4), suggesting that ice microphysics is crucial for moistening the midtroposphere. A comparison of RE and LI indicates that rain reevaporation is also an important source of midtropospheric moisture, while cloud liquid reevaporation is not (CE versus LI). Across all cases, *RH* shows a pronounced increase below 500 hPa owing to higher N_d (Figure 1h). With the exception of CE, they all experience lower *RH* in the upper troposphere.

Table 1
Domain-Average Column-Integrated Condensation (C), Total Reevaporation (E), Rain Reevaporation (ER), Cloud Condensate Reevaporation (EC), Accretion (AR), and Precipitation (P) in Different Cases

	C	E	ER	EC	AR	P	α	$\tilde{\delta\alpha}$
FU	13.7 (0.9)	9.1 (0.8)	3.7 (−0.7)	5.4 (1.5)	8.2 (−0.6)	4.5 (0.1)	0.664 (0.014)	0.022
LI	10.2 (1.1)	5.8 (1.0)	2.7 (−0.6)	3.1 (1.6)	7.1 (−0.5)	4.5 (0.1)	0.569 (0.033)	0.046
RE	7.6 (1.3)	2.8 (1.3)	0.5 (−0.2)	2.3 (1.4)	5.2 (−0.1)	4.7 (0.1)	0.368 (0.092)	0.108
CE	9.1 (0.5)	4.6 (0.5)	2.7 (−0.6)	2.0 (1.1)	7.1 (−0.6)	4.4 (0.0)	0.505 (0.026)	0.027

Note. Also included is the reevaporation efficiency (α). The differences between the control and perturbation simulations (the latter minus the former) are in parentheses. Except for α (unitless), all values are in mm day^{-1}. The last column ($\tilde{\delta\alpha}$) is based on a simple theory for $\delta\alpha$, that is, $(1-\alpha)\delta C/C$. The calculation for FU includes ice terms, as detailed in Table S1.

The impression from Figures 1f and 1h that convective invigoration coincides with midtropospheric moistening is formalized in Figure 2. The vertically averaged convective mass flux ($[M_c]$) in the various control and perturbation experiments is generally positively correlated with the column-averaged relative humidity (*CRH*). The correlation with the midtropospheric (400 to 600 hPa) relative humidity (*MRH*) is even stronger. This relationship holds not only for every pair of control and perturbation experiments but also for all the control experiments. Although it is well established that a moist midtroposphere is conducive to convective development (e.g., in the context of tropical cyclones), convective detrainment of cloud condensate is an important supplier of midtropospheric moisture. These two mechanisms are not mutually exclusive and work in the same direction. This work does not attempt to address the relative roles of these mechanisms, which would be difficult to separate in a clean way.

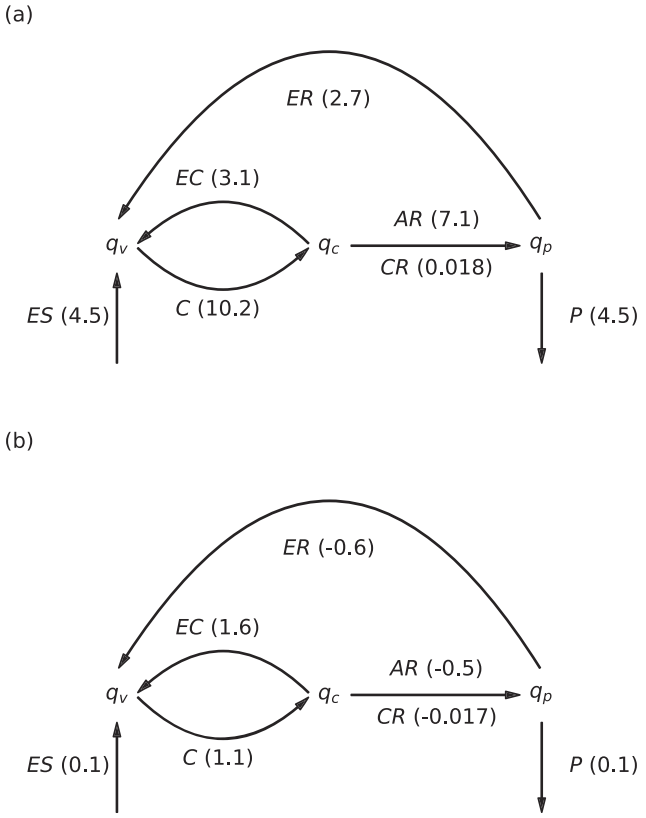

Figure 3. Domain-averaged column-integrated rates (mm day^{-1}) of microphysical processes involving water vapor (q_v), cloud condensates (q_c), and hydrometeors (q_p) (condensation of cloud condensates [*C*], reevaporation of cloud condensates [*EC*], conversion of cloud water to rain by autoconversion [*CR*] and accretion [*AR*], and reevaporation of rain [*ER*]), as well as surface evaporation (*ES*) and precipitation (*P*). Panel (a) is the LI control experiment, and (b) the difference between LI and LI*. The corresponding values for all configurations are listed in Table 1.

The need to better understand the controlling factors of *RH* prompts us to examine the moisture budget. The column-integrated source and sink terms, along with the changes caused by increased N_d, are given in Table 1. To facilitate the discussion, they are also illustrated in Figure 3 for the LI configuration. For water vapor, condensation (*C*) is balanced by surface evaporation (*ES*), and reevaporation of cloud condensate and rain (*EC* and *ER*, respectively). The conversion from cloud liquid to rain is realized through autoconversion (*CR*) and accretion (*AR*). Although autoconversion is almost negligible in terms of domain average (consistent with other cloud-resolving simulations e.g., Heikenfeld et al., 2019), it is the only process through which rain formation can occur spontaneously—a necessary condition for accretion that involves both cloud liquid and rain simultaneously. In this sense, it is conceivable that a perturbation to the former, however small in magnitude, may still affect the latter. Rain is partitioned between reevaporation (*ER*) and surface precipitation (*P*).

The reevaporation efficiency (α) is defined as the ratio of the total reevaporation (*E*, or the sum of *EC* and *ER*) to *C* (Romps, 2014). Note that one definition of the widely used quantity called precipitation efficiency is the ratio of surface precipitation (*P*) to *C* (e.g., Langhans et al., 2015; Lutsko & Cronin, 2018). Thus, α is one minus the precipitation efficiency. Dictated, to the zeroth order, by the prescribed free-tropospheric radiative cooling rate, the domain-average *ES* or *P* is little changed regardless of the configurations or perturbations. Both *C* and *E* are substantially lower in LI than in FU, but the fractional decrease in *E* is greater than that in *C*. This results in a net decrease in α. As expected, weakening the reevaporation processes tends to lower α, albeit to different extents. α is more sensitive to the perturbation to rain reevaporation than that to cloud liquid reevaporation, implying that *EC* is limited more strongly by the availability of cloud liquid as opposed to the prescribed rate constant.

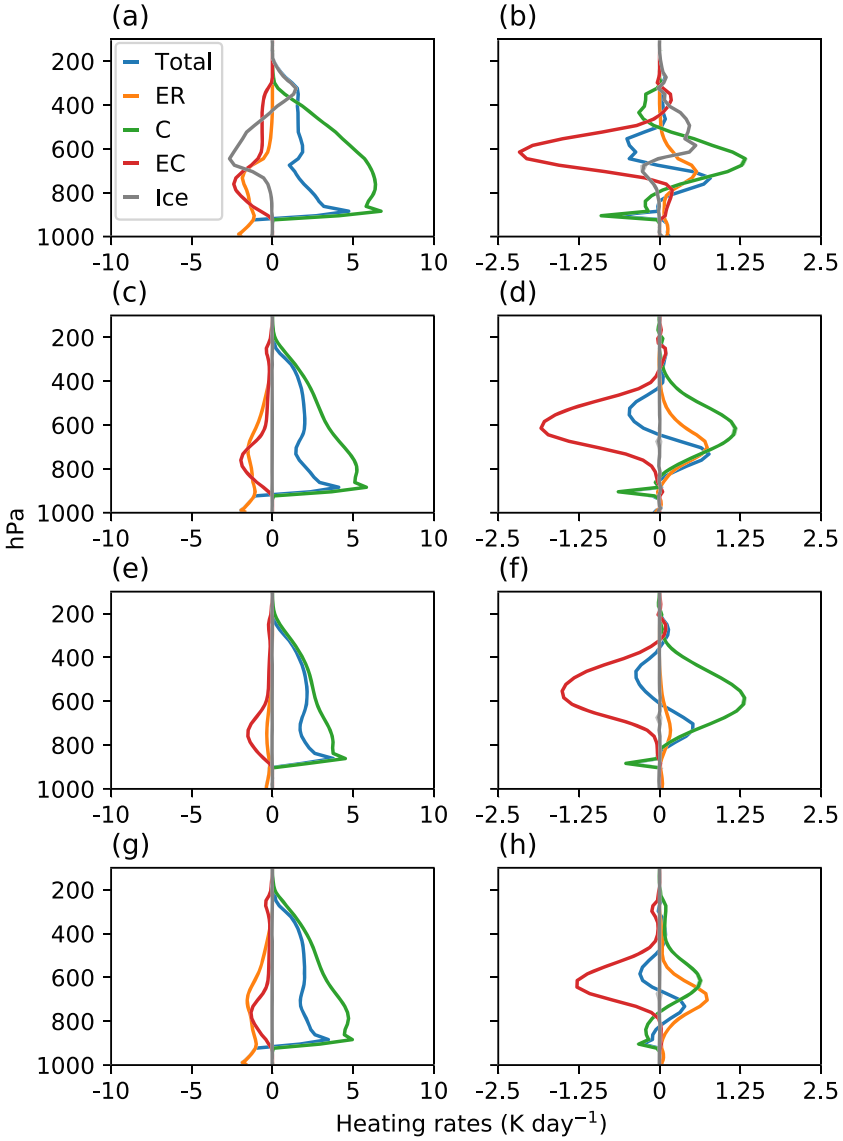

Figure 4. Vertical profiles of the domain-averaged heating rates (K day^{-1}) due to condensation (C), rain reevaporation (ER), cloud condensate reevaporation (EC), ice microphysics (Ice), and the total (Total). The control experiments are in the left column, and the difference between the control and perturbation experiments are in the right column. (a and b) FU, (c and d) LI, (e and f) RE, and (g and h) CE.

Higher N_d leads to a slowdown in accretion by modulating autoconversion. This is consistent with higher q_l and lower q_r (Figures 1b and 1d). As explained before, since P is somewhat fixed, and δCR is small, δAR must be approximately equal to δER (with δ denoting changes). This explains why rain reevaporation decreases. Higher q_l is consistent with stronger EC as they are directly linked. Since P is approximately unchanged, it follows that $\delta C \simeq \delta ER + \delta EC$. This relation, however, does not help constrain the sign of δC as δER and δEC are of opposite signs. It seems plausible to assume that C and EC would vary in the same direction as they are the dominant sink and source terms in the cloud liquid budget, an issue to which we will return later.

Invoking $\delta C \simeq \delta E$, one can write $\delta\alpha$ approximately as $(1-\alpha)\delta C/(C+\delta C)$. If it is assumed that $\delta C \ll C$, the expression can be further simplified to $\delta\alpha \simeq (1-\alpha)\delta C/C$. This simple theory is found to be in good agreement with the simulated $\delta\alpha$ (Table 1). Thus, the increase in α can be thought of as a manifestation of stronger condensation.

Across all the cases, α is strongly correlated with column relative humidity (*CRH*) (Figure 2c), and to a lesser extent, with midtropospheric relative humidity (*MRH*) (Figure 2d). This result is qualitatively consistent with an analytical model of tropospheric relative humidity in RCE (Romps, 2014), in which cloud condensate reevaporation is treated as an important mechanism for moistening the environment. In particular, α is smaller than *CRH*, conforming to the constraint inferred from the analytical model. This line of reasoning appears to suggest that the microphysical perturbation caused by higher N_d tends to increase the reevaporation efficiency. The resulting tropospheric moistening creates a favorable environment for convection.

As appealing as the above explanation is, it does not yield insights into the dynamics underlying the convective invigoration. The microphysical processes discussed above can be divided into two categories depending on whether phase change is involved. The latent heating from condensation (C) and the latent cooling from rain and cloud condensation reevaporation (*ER* and *EC*, respectively) play crucial roles in the energy balance, and have to be in equilibrium with other diabatic (e.g., radiative) and dynamical terms (resolved and implicit). In contrast, accretion is not part of the energy balance. Furthermore, the latent heating and cooling have distinct vertical structures as illustrated in Figure 4. In all the control experiments, the condensational heating peaks much lower (~900 hPa) than the reevaporative cooling (600 to 700 hPa). Conceptually, the former generates positive buoyancy for lifting an air parcel. As the parcel rises, it entrains drier/colder environmental air and detrains cloud condensate, which then reevaporates into the environment. Similar to condensation, the total heating is bottom-heavy, but with a distinct local minimum owing to reevaporation.

Both condensation and cloud liquid reevaporation are stronger in the perturbed energy balance, with a secondary weakening of rain reevaporation. Although the combined effect is integrated vertically to near 0, it is characteristic of a dipole (cooling above warming) structure as δC is more bottom-heavy than δEC. The positive buoyancy resulting from this pattern is consistent with the enhancement of M_c (Figure 1f). Given that the initial perturbation is applied through modifying cloud liquid, one may speculate that it is the stronger reevaporative cooling that destabilizes the lower troposphere and promotes stronger convection (condensation). This explains why condensation and cloud liquid reevaporation vary in the same direction, and constitutes a dynamical mechanism of the microphysically induced convective adjustment.

4. Discussion and Conclusions

As an anchor point of this work, the reevaporation efficiency (α) is an emergent property of the RCE simulations and is closely associated with tropospheric relative humidity and convective mass fluxes across a wide range of model configurations and perturbations. It has been shown that the increase in α due to higher N_d can be linked to stronger condensation by invoking the simple theory ($\delta\alpha \simeq (1-\alpha)\delta C/C$), which can also be used to explain, at least qualitatively, the large difference in α among the four control experiments (from 0.368 in RE to 0.664 in FU). Although it is clear from our results that the treatment of cloud microphysics has a direct bearing on α, convective dynamics also plays an essential role, as evidenced by the destabilizing effect of cloud liquid reevaporation. In light of its importance for understanding tropospheric relative humidity (Romps, 2014), convectively coupled tropical variations and general circulation (Emanuel, 2019) and climate sensitivity (Zhao et al., 2016), the potential use of α for comparing a variety of model simulations (limited-domain and global CRMs, and coarse-resolution global climate models or GCMs) and observations (Noone, 2012) should be explored.

A contemporaneous study by Abbott and Cronin (2020) offers a way to examine the robustness of our results to the choice of model configurations and experimental designs. Both studies find that an increase in N_d gives rise to higher mid-tropospheric relative humidity and convective invigoration in RCE simulations, even in the absence of ice microphysics. While this work centers over convective invigoration (manifested as stronger convective mass flux) in RCE, Abbott and Cronin (2020) focuses on changes in high-percentile vertical velocities under the assumption of weak temperature gradient balance.

Unlike bin-based cloud microphysics schemes with explicit supersaturation, the bulk scheme used in this work is based on the assumption of saturation adjustment, meaning that any water vapor in excess of saturation is converted into cloud condensates. As such, this scheme does not take into account the dependence of supersaturation and condensational growth of droplets on aerosol concentrations (Dagan et al., 2015; Pinsky et al., 2013; Seiki & Nakajima, 2014), nor the full range of droplet effective terminal velocities (Koren et al., 2015). Yet, it has been shown that increased aerosols can delay rain formation and invigorate

individual warm clouds by reducing condensational growth and effective terminal velocities (Koren et al., 2014). Neither factor is fully considered in this work. It is, nonetheless, important to note that this shortcoming does not affect the validity of the physical mechanisms identified in this work, which are different from those in Koren et al. (2014). Furthermore, as mentioned in the introduction, it is difficult to draw a meaningful comparison between case studies like Koren et al. (2014) and RCE-based studies like ours.

Ice microphysical processes are often thought to play a key role in enhancing convection under polluted conditions. In the setting of RCE with prescribed radiative cooling, we demonstrate that an increase in cloud droplet number concentration can cause stronger convective mass flux even in the absence of ice microphysics. Subsequent sensitivity tests of liquid microphysical processes indicate that cloud liquid reevaporation plays a more important role in driving the convective invigoration than rain reevaporation. A process-level analysis reveals that higher cloud droplet number concentration slows down the conversion of cloud liquid to rain, giving rise to an increase in cloud liquid reevaporation and a decrease in rain reevaporation, with the former outweighing the latter. The net increase in the total reevaporation is balanced by stronger condensation. The dipole pattern of reevaporative cooling above condensational heating is consistent with the enhancement of convective mass flux.

Data Availability Statement

Data and scripts used in this paper are available at https://doi.org/10.5281/zenodo.4068037.

Acknowledgments
We thank Tristan Abbott, Tim Cronin, Nadir Jeevanjee, Hugh Morrison, Ming Zhao, Hailey Shin, Usama Anber, Spencer Clark, and the two reviewers for helpful discussions, Shuguang Wang for providing the source code for the WRF model used in this study, and the developers of the "aospy" package. XRC was funded by the Cooperative Institute for Modeling the Earth System (CIMES) at Princeton University and the Singapore National Research Foundation.

References

Abbott, T. H., & Cronin, T. W. (2020). A humidity-entrainment mechanism for microphysical invigoration of convection. arXiv2002.06056.
Albrecht, B. A. (1989). Aerosols, cloud microphysics, and fractional cloudiness. *Science*, *245*(4923), 1227.
Andreae, M. O., Rosenfeld, D., Artaxo, P., Costa, A. A., Frank, G. P., Longo, K. M., & Silva-Dias, M. A. F. (2004). Smoking rain clouds over the Amazon. *Science*, *303*(5662), 1337–1342.
Chua, X. R., Ming, Y., & Jeevanjee, N. (2019). Investigating the fast response of precipitation intensity and boundary layer temperature to atmospheric heating using a cloud-resolving model. *Geophysical Research Letters*, *46*, 9183–9192. https://doi.org/10.1029/2019GL082408
Dagan, G., Koren, I., & Altaratz, O. (2015). Competition between core and periphery-based processes in warm convective clouds-from invigoration to suppression. *Atmospheric Chemistry & Physics*, *15*(5), 2749–2760.
Emanuel, K. (2019). Inferences from simple models of slow, convectively coupled processes. *Journal of the Atmospheric Sciences*, *76*(1), 195–208. https://doi.org/10.1175/JAS-D-18-0090.1
Fan, J., Rosenfeld, D., Yang, Y., Zhao, C., Leung, L. R., & Li, Z. (2015). Substantial contribution of anthropogenic air pollution to catastrophic floods in Southwest China. *Geophysical Research Letters*, *42*, 6066–6075. https://doi.org/10.1002/2015GL064479
Fan, J., Rosenfeld, D., Zhang, Y., Giangrande, S. E., Li, Z., Machado, L. A. T., et al. (2018). Substantial convection and precipitation enhancements by ultrafine aerosol particles. *Science*, *359*(6374), 411–418.
Fan, J., Yuan, T., Comstock, J. M., Ghan, S., Khain, A., Leung, L. R., et al. (2009). Dominant role by vertical wind shear in regulating aerosol effects on deep convective clouds. *Journal of Geophysical Research*, *114*, D22206. https://doi.org/10.1029/2009JD012352
Heikenfeld, M., White, B., Labbouz, L., & Stier, P. (2019). Aerosol effects on deep convection: The propagation of aerosol perturbations through convective cloud microphysics. *Atmospheric Chemistry and Physics*, *19*(4), 2601–2627.
Hong, S.-Y., Noh, Y., & Dudhia, J. (2006). A new vertical diffusion package with an explicit treatment of entrainment processes. *Monthly Weather Review*, *134*(9), 2318–2341.
Jiang, H., & Feingold, G. (2006). Effect of aerosol on warm convective clouds: Aerosol-cloud-surface flux feedbacks in a new coupled large eddy model. *Journal of Geophysical Research*, *111*, D01202. https://doi.org/10.1029/2005JD006138
Khairoutdinov, M., & Kogan, Y. (2000). A new cloud physics parameterization in a large-eddy simulation model of marine stratocumulus. *Monthly Weather Review*, *128*(1), 229–243.
Koren, I., Altaratz, O., & Dagan, G. (2015). Aerosol effect on the mobility of cloud droplets. *Environmental Research Letters*, *10*(10), 104011.
Koren, I., Dagan, G., & Altaratz, O. (2014). From aerosol-limited to invigoration of warm convective clouds. *Science*, *344*(6188), 1143–1146.
Langhans, W., Yeo, K., & Romps, D. M. (2015). Lagrangian investigation of the precipitation efficiency of convective clouds. *Journal of the Atmospheric Sciences*, *72*(3), 1045–1062.
Lutsko, N. J., & Cronin, T. W. (2018). Increase in precipitation efficiency with surface warming in radiative-convective equilibrium. *Journal of Advances in Modeling Earth Systems*, *10*, 2992–3010. https://doi.org/10.1029/2018MS001482
Morrison, H. (2012). On the robustness of aerosol effects on an idealized supercell storm simulated with a cloud system-resolving model. *Atmospheric Chemistry and Physics*, *12*(16), 7689–7705.
Morrison, H., Thompson, G., & Tatarskii, V. (2009). Impact of cloud microphysics on the development of trailing stratiform precipitation in a simulated squall line: Comparison of one-and two-moment schemes. *Monthly Weather Review*, *137*(3), 991–1007.
Noone, D. (2012). Pairing measurements of the water vapor isotope ratio with humidity to deduce atmospheric moistening and dehydration in the tropical midtroposphere. *Journal of Climate*, *25*(13), 4476–4494.
Pinsky, M., Mazin, I. P., Korolev, A., & Khain, A. (2013). Supersaturation and diffusional droplet growth in liquid clouds. *Journal of the Atmospheric Sciences*, *70*(9), 2778–2793.
Romps, D. M. (2014). An analytical model for tropical relative humidity. *Journal of Climate*, *27*(19), 7432–7449.
Rosenfeld, D., Lohmann, U., Raga, G. B., O'Dowd, C. D., Kulmala, M., Fuzzi, S., et al. (2008). Flood or drought: How do aerosols affect precipitation? *Science*, *321*(5894), 1309–1313.
Seifert, A., Heus, T., Pincus, R., & Stevens, B. (2015). Large-eddy simulation of the transient and near-equilibrium behavior of precipitating shallow convection. *Journal of Advances in Modeling Earth Systems*, *7*, 1918–1937. https://doi.org/10.1002/2015MS000489

Seiki, T., & Nakajima, T. (2014). Aerosol effects of the condensation process on a convective cloud simulation. *Journal of the Atmospheric Sciences*, *71*(2), 833–853.
Stevens, B., & Feingold, G. (2009). Untangling aerosol effects on clouds and precipitation in a buffered system. *Nature*, *461*(7264), 607.
Storer, R. L., & van den Heever, S. C. (2013). Microphysical processes evident in aerosol forcing of tropical deep convective clouds. *Journal of the Atmospheric Sciences*, *70*(2), 430–446.
Tao, W.-K., Chen, J.-P., Li, Z., Wang, C., & Zhang, C. (2012). Impact of aerosols on convective clouds and precipitation. *Reviews of Geophysics*, *50*, RG2001. https://doi.org/10.1029/2011RG000369
Tao, W.-K., Li, X., Khain, A., Matsui, T., Lang, S., & Simpson, J. (2007). Role of atmospheric aerosol concentration on deep convective precipitation: Cloud-resolving model simulations. *Journal of Geophysical Research*, *112*, D24S18. https://doi.org/10.1029/2007JD008728
Twomey, S. (1974). Pollution and the planetary albedo. *Atmospheric Environment*, *8*(12), 1251–1256.
van den Heever, S. C., Stephens, G. L., & Wood, N. B. (2011). Aerosol indirect effects on tropical convection characteristics under conditions of radiative–convective equilibrium. *Journal of the Atmospheric Sciences*, *68*(4), 699–718.
Wang, S., & Sobel, A. H. (2011). Response of convection to relative sea surface temperature: Cloud-resolving simulations in two and three dimensions. *Journal of Geophysical Research*, *116*, D11119. https://doi.org/10.1029/2010JD015347
Williams, E., Rosenfeld, D., Madden, N., Gerlach, J., Gears, N., Atkinson, L., et al. (2002). Contrasting convective regimes over the Amazon: Implications for cloud electrification. *Journal of Geophysical Research*, *107*(D20), 8082. https://doi.org/10.1029/2001JD000380
Xue, H., & Feingold, G. (2006). Large-eddy simulations of trade wind cumuli: Investigation of aerosol indirect effects. *Journal of the Atmospheric Sciences*, *63*(6), 1605–1622.
Zhao, M., Golaz, J.-C., Held, I. M., Ramaswamy, V., Lin, S.-J., Ming, Y., et al. (2016). Uncertainty in model climate sensitivity traced to representations of cumulus precipitation microphysics. *Journal of Climate*, *29*(2), 543–560.